ECOCYCLES
ISSN 2416-2140

OPEN ACCESS
Scientific journal of the
European Ecocycles Society

Ecocycles, Vol. 10, No. 2, pp. 80-95 (2024)
DOI: 10.19040/ecocycles.v10i2.490

RESEARCH ARTICLE

Acoustic Performance of Mesoporous Charcoal: A Comparative Study Using Impedance Tube, Anechoic Chamber, and Mass Law

Olga Khrystoslavenko [1], M. Usman Sikandar [2]

[1] *Department of Environmental Protection and Water Engineering, Vilnius Tech, Vilnius, Lithuania*
[2] *Faculty of Mechanical Engineering and Design, Institute of Mechatronics, KTU Kaunas, Lithuania*
Corresponding author: M. Usman Sikandar *email:* muhsik@ktu.lt

Abstract – As the demand for sustainable materials in acoustic applications grows, mesoporous charcoal—produced via biomass pyrolysis—has emerged as a promising material for acoustic absorption and thermal insulation. This study investigates its acoustic properties using impedance tube and anechoic chamber measurements, alongside comparisons with mass law predictions. Charcoal samples, characterized by pore sizes ranging from 2 to 50 nm and fraction sizes from 1 to 4 cm, were tested across varying thicknesses (5 cm, 10 cm, and 17 cm) and frequencies (315 Hz to 5000 Hz). The Johnson-Champoux-Allard-Lafarge (JCAL) model was used to derive key acoustic parameters. These parameters were instrumental in explaining the material's behaviour in different acoustic environments. Impedance tube measurements revealed sound absorption coefficients below 0.1 for most samples, attributed to the material's low porosity ($\phi = 0.19$) and fine pore structure. In contrast, anechoic chamber tests demonstrated increased sound reduction, with a 17 cm thick construction (fraction size 1 cm) achieving a sound reduction index (SRI) of 35 dB at 5000 Hz, significantly exceeding the transmission loss (TL) predicted by mass law, which calculated a TL of only 8.28 dB under similar conditions. Statistical analysis further revealed that SRI increases with particle size and thickness, ranging from 9.17 for 1 cm particles to 18.38 for 4 cm particles. The highest SRI of 28.00 was observed for 1 cm particles at 17 cm thickness, while bulk density results highlighted an inverse relationship with particle size: 1 cm particles had a bulk density of 550 kg/m³ compared to 323.33 kg/m³ for 4 cm particles. These findings highlight mesoporous charcoal's potential in sustainable acoustic applications, particularly in the context of circular economy principles. Its production from biomass, combined with the eco-friendly properties it brings to noise insulation, aligns with the goals of sustainable material cycles. Optimizing parameters such as pore size, fraction size, and thickness can further increase its acoustic performance, making it a promising material for eco-friendly construction and noise control.

Keywords – Sound reduction index, wood charcoal, sound absorbing materials, anechoic chamber, impedance tube, Johnson–Champoux–Allard–Lafarge model, Mass Law, sustainable material cycles

Received: October 15, 2024 Accepted: December 2, 2024

1. INTRODUCTION

The growing issue of environmental pollution worldwide highlights the urgent need to develop eco-friendly materials sourced from natural resources. There is increasing interest in using natural and recycled materials in building construction (Aprianti, 2015; Patnaik, 2015; Estanqueiro, 2018). Porous absorbing materials have demonstrated the ability to absorb a significant portion of sound energy while reflecting minimal amounts, making them highly effective tools for noise control (Arenas & Crocker, 2010). Research has focused on porous sound-absorbing materials (Liu et al., 2016; Bruijn et al., 2016; Berardi et al., 2015; Chen, 2016). For instance, cellulose aerogels have become a sustainable and effective acoustic material due to their porous structures, with freeze-drying techniques increasing their sound absorption properties, especially at low-mid frequencies (Ruan et al., 2024).

The construction of sound absorption materials has been, with studies exploring various methodologies and materials (Wen et al., 2011; Yilmaz et al., 2011). Sound-absorbing materials depend heavily on their porosity. The standard metric to quantify their effectiveness is the absorption coefficient, which ranges from 0 to 1.0, with 0 being perfectly

non-absorbent and 1.0 indicating 100% absorption. Since materials absorb sound more effectively at specific frequencies, absorption coefficient values are typically given as a function of frequency (Nandanwar, 2017). Sound-absorbing materials absorb most of the sound energy striking them and reflect very little. The material structure significantly influences sound absorption; open pores absorb sound better than closed pores. Figure 1 shows a schematic cross-section of a porous solid material. Pores entirely isolated from their neighbours are termed "closed" pores (Arenas & Crocker, 2010). Materials like granulated charcoal made from wood waste also shown significant sound absorption properties, influenced by a few factors such as grain size and bulk density, which were found superior in specific wood species like birch (Khrystoslavenko et al., 2023). Figure 1 illustrates a schematic cross-section of a porous solid material. The pores that are completely isolated from adjacent pores are referred to as 'closed' pores.

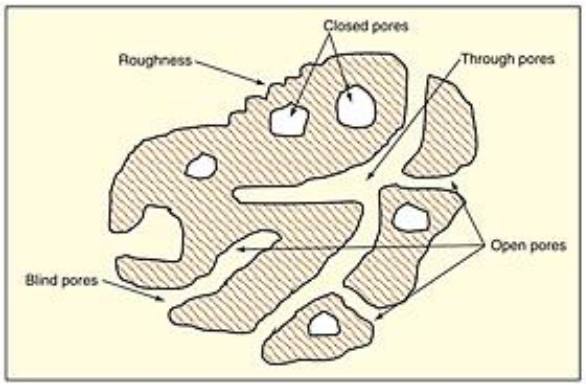

Fig. 1 Schematic cross-section of a porous solid material (Arenas and Crocker 2010)

Charcoal, widely used in art and medicine, can also be used as a filter due to its porous surface. It can be converted into activated carbon, resulting in a material that is soft, brittle, lightweight, black, and porous resembling coal (Gunner, 2016). Charcoal can be produced from biomass sources such as wood, woody agricultural products, the biogenic fraction of municipal waste, nutshells, and more. While the liquid and gaseous fractions derived from biomass are valuable fuel sources, the solid fraction (charcoal) has potential applications as carbon black or as a carbon adsorbent after undergoing an activation step. Charcoal is produced by slow heating of wood (carbonization) in airtight ovens, retorts, or kilns supplied with controlled amounts of air. It has the potential to increase soil properties, increase crop productivity, and contribute to carbon sequestration in soil. Typically, charcoal is produced by slow pyrolysis, which involves heating wood or other substances and in the absence of oxygen. (Demirbas, 2016).

Suh et al. (2013) studied the preparation of charcoal, noting that the carbonization process occurred at temperatures between 600 and 700 °C in over five days. Their research indicates that factors such as surface area, particle size, porosity, low density, specific heat, and electrical conductivity significantly influence sound absorption. The activated charcoal increases the sound absorption coefficient compared to non-carbon charcoal and has a surface area ranging from 500 to 1500 m^2/g due to its higher microporosity. The density of activated charcoal varies between 0.2 and 0.6 t/m^3, depending on the raw material used. Additionally, charcoal's bulk density is primarily influenced by its apparent density and particle size distribution, typically ranging from 180 to 220 kg/m^3. Its porosity was determined by both the feedstock and the pyrolysis conditions. (Arenas & Sakagami, 2020).

Despite its potential, there is limited research focused on the use of charcoal for sound absorption. Charcoal shows lower sound absorption properties compared to conventional materials such as fibreglass or non-woven fabrics (Suh et al., 2013). Arenas (2010) explained that sound waves hitting the surface of porous materials cause the air inside the pores to oscillate. As air passes through the pores, a portion of the sound energy is converted into heat due to thermal and viscous losses along the internal walls of the material's pores and channels (Arenas, 2010). Recent studies on sustainable charcoal and its composites show promising sound absorption performance when fabricated with different thicknesses and densities (Sakthivel et al., 2021; Janlee & Srisiriwat, 2023).

Charcoal is a homogeneous, rigid, porous material, which is why the semi-phenomenological Johnson–Champoux–Allard–Lafarge (JCAL) model is often used to describe its geometric pore structure. This model incorporates six non-acoustic parameters: porosity (ϕ), tortuosity (α_∞), viscous (Λ) and thermal (Λ') characteristic lengths, and static viscous and thermal permeability (k_0) and (k_0). The porous medium is treated as an equivalent fluid, characterized by an equivalent dynamic density ($\tilde{\rho}_{eq}$) and dynamic bulk modulus ($\tilde{K}_{eq}$), both of which are frequency-dependent and complex-valued. The sound absorption coefficient, sound transmission loss, effective density, and effective bulk modulus can be derived from these measured properties, along with the material's open porosity (Doutres et al., 2010).

Classical methods for evaluating non-acoustic properties of porous materials fall into three categories: first direct methods based on the physical definition of the property second indirect methods that link material properties to acoustic measurements through acoustic models, and third category is inverse methods where properties are adjusted to match acoustic measurements. This study exclusively uses indirect and inverse methods using impedance tube measurements (Doutres et al., 2010).

Atalla and Panneton (2005) demonstrated how open porosity and static airflow resistivity can be measured

directly, while dynamic density can be obtained using acoustical techniques involving impedance tubes. Analytical solutions derived from the Johnson et al. model provide geometric tortuosity and viscous characteristic length (Atalla & Panneton, 2005). Zielinski (2015) described a methodology for the inverse characterization of sound-absorbing rigid porous media. The sound absorption coefficient (SAC), which characterizes sound propagation in charcoal, is critical for optimizing and designing noise control devices (Yang et al., 2005). In this article, we define this parameter using an indirect method.

In Lee Hyung Ho's study, wood charcoal was used in building interiors such as windows, doors, and partition walls, which effectively improved noise isolation and reduced internal reverberation. Lee further explored charcoals sound absorption structure and its application in creating charcoal board-wood composites with a natural wood finish. This composite allows one or both surfaces of activated carbon or charcoal boards to show adsorption properties, absorbing radon gas from concrete walls or other gases indoors (Lee, 2016). Moreover, charcoal's ability to act as an acoustic diffuser has been demonstrated by increasing sound reflection through impedance tube measurements (Khrystoslavenko & Grubliauskas, 2022).

Matsumura developed a sound-absorbing structure with a gas adsorption material enclosed in a housing. This structure reduces size while achieving sound absorption, particularly in low frequency ranges (Matsumura, 2006). The goal of this study is to investigate the sound absorption properties of charcoal using impedance tube and anechoic chamber techniques and calculation of mass effect through mass law. Structure of charcoal was defined, revealing a microstructure in which porosity depends primarily on the source material (HWANG & OH, 2024; Khrystoslavenko & Grubliauskas, 2022).

The aim of this paper is to research the sound absorption properties of mesoporous charcoal-based constructions and evaluate its sound insulation performance across a wide frequency range.

2. MATERIALS AND METHODS

The techniques employed for measurement included impedance tube and anechoic chamber methods. The impedance tube method, thoroughly described in ISO 10534-2 (ISO 10534-2:1998, 1998), is commonly used to characterize porous materials. Acoustic impedance data, such as transmission and reflection, were collected using the impedance tube.

The design characteristics of the tube are illustrated in Figure 2. Microphones are placed between the loudspeaker and the sample. A loudspeaker, controlled by a signal source, generates a one-dimensional wave that transmits sound energy directly through the sample. The impedance tube consists of four microphones and is terminated with an anechoic end featuring two microphones. Two 1/4-inch G.R.A.S. microphones are positioned on either side. The tube's diameter is 30 mm, with the distances between microphones 1-2 and 3-4 measuring 20 mm. The distance from microphone 2 to the sample surface is 30 mm, while the distance from the sample surface to microphone 3 is 150 mm. Signal excitation was achieved using a logarithmic enveloped sine wave within the frequency range of 300-5800 Hz (Niskanen et al., 2017).

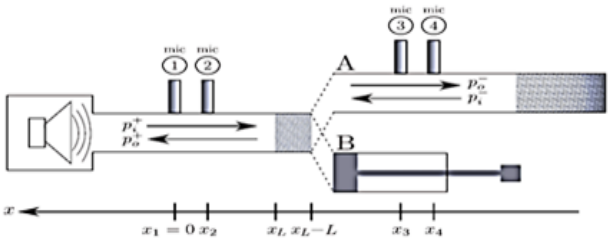

Fig. 2 Impedance tube, A: transmission set-up. B: rigid backing

The impedance tube was calibrated before conducting the measurements to account for any microphone phase incompatibility. This calibration process included fine-tuning the position of the microphones to ensure accurate results.

The objects of study are presented in Figure 3. Charcoal, a homogeneous, solid isotropic porous material, demonstrates significant potential for use in the development of noise-protective barriers. An experiment was carried out in the impedance tube with a charcoal sample, measuring 25 mm in thickness to analyse its acoustic properties and performance in sound absorption.

Fig.3 Sample of charcoal material
(Thickness 25 mm; diameter 30 mm)

The scattering matrix, which includes the reflection and transmission coefficients (R and T) of a homogeneous symmetric plate, can be derived from measurements taken using a four-microphone impedance tube. Subsequently, the equivalent dynamic density ($\tilde{\rho}_{eq}$) and the equivalent bulk modulus ($\tilde{K}_{eq}$) can be calculated directly (Niskanen et al., 2017).

$$P_1 = p_i^+ e^{iktx1} + p_0^+ e^{-iktx1}, \quad (1)$$

$$P_2 = p_i^+ e^{iktx2} + p_0^+ e^{-iktx2}, \quad (2)$$

$$P_3 = p_0^- e^{iktx3} + p_0^- e^{-iktx3}, \quad (3)$$

$$P_4 = p_0^- e^{iktx4} + p_0^- e^{-iktx4}, \quad (4)$$

Where*:*
Pj - sound pressures at locations x_j, j=1, 2, 3, 4;
p – standing waves inside the tube on the left and right surfaces of the sample,
i – incoming waves in relation to the sample;
o "outgoing" waves in relation to the sample;
plus - "left" sides of the sample in the tube;
minus - "right" sides of the sample in the tube;
k_t - wavenumber;
Z_t - characteristic impedance: ρ_0 - density of air

The Zwikker and Kosten formulas were used to calculate the wavenumber (k_t) and characteristic impedance (Z_t), accounting for the viscothermal effects at the boundary of the impedance tube (Niskanen et al., 2017). These formulas are crucial for accurately modelling the propagation of sound waves through the tube and characterizing the impedance properties of the tested materials.

$$\rho_0 = \frac{P_0}{RH \times T0} \quad (5)$$

Where*:*
P0 - atmospheric pressure,
T0, - temperature
RH – relative humidity, from which the density of air
ρ_0 can be calculated.

The scattering matrix can be written as

$$\begin{bmatrix} p_0^+ \\ p_0^- \end{bmatrix} = \begin{bmatrix} R & T \\ T & R \end{bmatrix} \begin{bmatrix} p_0^+ \\ p_0^- \end{bmatrix}, \quad (6)$$

Where:
R = reflection;
$T_0 = T^{ik_t L}$ transmission coefficients of a symmetric porous sample
L - thickness of the sample.
p_0^+ - standing wave pressures "left" sides of the sample in the tube;
p_0^- - standing wave pressures "right" sides of the sample in the tube.

The pressures (p) in the scattering matrix (Eq. 6) represent the standing wave pressures on the left and right surfaces of the sample. To determine these pressures, the standing wave amplitudes at position x1 are solved using Equations 1, 2, 3, and 4, and the resulting pressures are multiplied by the appropriate propagation constant, depending on the distance to the surface (Niskanen et al., 2017). This process allows for an accurate determination of the pressures acting on the surfaces of the sample, which are essential for calculating the scattering matrix and characterizing the acoustic properties of the material.

$$P = \frac{P_1 e^{-iktx1} - P_2 e^{-iktx2}}{e^{-2iktx1} - e^{-2iktx2}} e^{-ik_t|x_L|} \quad (7)$$

$$P = \frac{P_1 e^{-iktx1} - P_2 e^{-iktx2}}{e^{-2iktx1} - e^{-2iktx2}} e^{-ik_t|x_L|} \quad (8)$$

$$P = \frac{P_1 e^{-iktx1} - P_2 e^{-iktx2}}{e^{-2iktx1} - e^{-2iktx2}} e^{-ik_t(|x_L|+L)} \quad (9)$$

$$P = \frac{P_1 e^{-iktx1} - P_2 e^{-iktx2}}{e^{-2iktx1} - e^{-2iktx2}} e^{-ik_t(|x_L|+L)} \quad (10)$$

Transmission and reflection coefficients for the symmetric porous sample can be solved from Eq. 11,12

$$T = \frac{p_0^- p_i^+ - p_0^+ p_i^-}{(p_0^+)^2 - (p_i^-)^2} \quad (11)$$

$$R = \frac{p_0^+ p_i^+ - p_0^- p_i^-}{(p_0^+)^2 - (p_i^-)^2} \quad (12)$$

The scattering matrix would include reflection coefficients R^+ and R^- if the material was non-symmetric, from both sides of the sample. The characteristic impedance (Z_m) and wavenumber (k_m) of the material can be writing as,

$$Z_m = Z_t \sqrt{\frac{(1+R)^2 - T^2}{(1-R)^2 - T^2}} \quad (13)$$

$$e^{-ikmL} = \frac{T(1+R)^2 - T^2}{R(1-\tilde{z}) - \tilde{z} + 1} \quad (14)$$

$$\Rightarrow k_m = -\frac{\ln(|e^{-iktx1}| + iArg(e^{-ikmL})(e^{-ikmL}))^2}{iL} + \frac{2\pi n}{iL} \quad (15)$$

Where:
Z_m/Z_t and n ∈ ℕ. The term 2πn exists to account for the phase wrap when inverting the k_m. Usually *n* is 0 because the measurements are performed in the low frequency range. Then, we get

$$\tilde{\rho}_{eq} = Z_m k_m / \omega \quad (16)$$

$$\tilde{K}_{eq} = Z_m \omega / k_m \quad (17)$$

Niskanen et al. provided a detailed description of the technique and measurement configuration used in this research (Niskanen et al., 2017).

The Johnson et al. model is used to describe the dynamic density of a porous medium, while the Champoux–Allard–Lafarge model is applied to explain the dynamic bulk modulus (Champoux & Allard, 2013; Lafarge et al., 1997; Johnson et al., 1987; Johnson et al., 1986).

Bulk modulus and equivalent density are key parameters in characterizing the acoustic behaviour of porous materials. The bulk modulus reflects a material's resistance to compression, while the equivalent density represents the mass per unit volume. Both parameters are vital for modelling and understanding the sound absorption properties of porous media (ISO 9053:1991).

$$\tilde{K}_{eq(\omega)} = \gamma P_0 \left(\gamma - \frac{(\gamma-1)}{\left[1+\frac{\sigma\phi}{i\alpha_\infty \rho_0 N_{Pr}\omega\left(1+\frac{4i\alpha_\infty^2 \eta\rho_0 N_{Pr}\omega}{\sigma^2\Lambda^2\phi^2}\right)}\right]^{1/2}} \right)^{-1} \quad (18)$$

Where:
η is the viscosity of air,
γ is the specific heat ratio of air,
P_0 is the air equilibrium pressure,
ρ_0 is the density of air, and
N_{Pr} is the Prandtl number equivalent density:

$$\tilde{\rho}_{eq}(\omega) = \rho_0 \alpha_\infty \left[1 + \frac{\sigma\phi}{i\alpha_\infty \rho_0 \omega}\left(1 + \frac{4i\alpha_\infty^2 \eta\rho_0\omega}{\sigma^2\Lambda^2\phi^2}\right)\right]^{1/2} \quad (19)$$

In the study by Niskanen et al. (2017), the equivalent density and bulk modulus of the samples are reconstructed using the scattering matrix formalism, which is then linked to their physical parameters using the Johnson–Champoux–Allard–Lafarge model.

The absorption coefficient was defined based on impedance tube measurements and calculated using the equation:

$$\alpha = 1 - |R|^2 \quad (20)$$

Where:
α - absorption coefficient;
R - reflection coefficients

The research was conducted in a VILNIUS TECH anechoic chamber within a volume of 10.8 m³, Department of Environmental Protection. The laboratory chamber consists of two rooms separated by a double wall, with an adjacent room designated for measuring equipment (see Fig. 4).

Room 1, commonly referred to as the source room, is responsible for transmitting sound, while Room 2 serves as the target room for receiving the sound. The sample has a volume (V) of 0.10 m³, with both the source and receiving rooms having a volume of 5.4 m³ of each room.

The instrument used for measurements is equipped with two channels, enabling noise recording at different points simultaneously through two microphones. One microphone is placed in the source room, and the other in the target room. One method used for these measurements is the microphone doublet method, which is effective at low frequencies but requires a sound source, like a loudspeaker, to be mounted at an appropriate distance (Grubliauskas & Butkus, 2009).

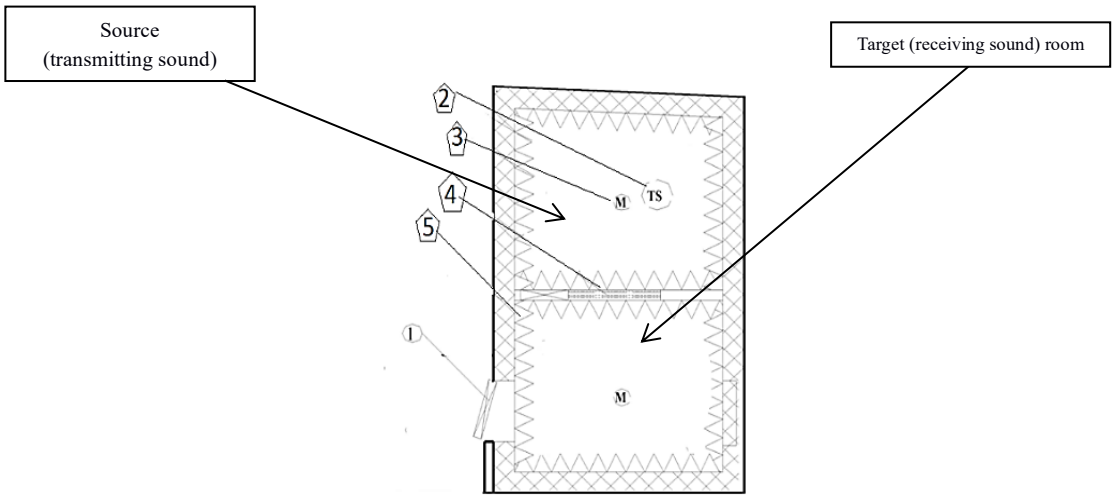

Fig. 4 Situation plan of the anechoic chamber; view from above the noise-suppression chamber:
1 – Door; 2 – Positions of noise sources (TS); 3 – Microphone positions (M); 4 – Cage for mounting the study samples; PP – Data-recording-&-processing room; 5 - Layer of acoustic foam.

The equipment used to measure the sound reduction index included the Sound Level Analyzer Bruel & Kjaer 2260, the Spectrum Analyzer Bruel & Kjaer Mediator 2260, the Bruel & Kjaer 4189 microphone, and Bruel & Kjaer program software.

In the anechoic chamber, sound propagated from the source into the propagation room. The construction, as shown in Fig. 5, used charcoal with varying fraction sizes (1, 2, 3, and 4 cm). These fractions were chosen to compare how material density affects sound absorption.

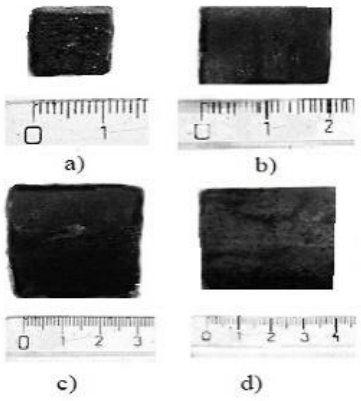

Fig. 5 Sample of charcoal materials: size of fraction
a)1; b) 2; c) 3; d) 4 cm

Measurements were carried out across a frequency range of 315 to 5000 Hz. Figure 6 shows the completed construction filled with charcoal. Different construction thicknesses (5 cm, 10 cm, and 17 cm) were selected to explore how thickness affects the sound absorption properties. The goal was to identify a compact design with optimal acoustic performance. The selected thicknesses were based on the cage's construction, which has a diameter of 20 cm.

Fig. 6 Example condition in anechoic chamber

The charcoal particles in this fraction do not pack tightly together, leaving free space between them. The primary material in the composite is charcoal. The construction consists of a wooden frame, charcoal, and an iron mesh.

The mass law equation used to calculate the Transmission Loss (TL) in this study is derived from the general sound transmission theory for homogeneous barriers (Fahy, 2000). The equation predicts the TL based on the surface mass density of the material and the frequency of the sound waves:

$$TL = 20 \log_{10} \left[\frac{m.f}{p_o.c}\right] - 47 \quad (21)$$

Where:
TL - transmission loss in decibels (dB),
m - surface mass density of the material (kg/m²),
f - frequency of the sound wave (Hz),
ρ_0 - density of air (~1.21 kg/m³),
c - speed of sound in air
m is calculated by multiplying the material's bulk density (ρ) by the thickness of the material:

$$m = \rho \times t \quad (22)$$

To apply this equation, the bulk density of the material (in kg/m³) and the thickness (in meters) are used to calculate the surface mass density. The frequency of interest is then plugged into the mass law equation to predict the transmission loss. This calculated TL is compared with the experimentally measured Sound Reduction Index (SRI) to evaluate how well the material performs in practice compared to theoretical predictions. The mass law predicts TL based solely on the mass of the material, so any significant discrepancies between TL and SRI suggest additional factors, such as material structure and porosity, influence sound

insulation. This theoretical basis is well established in acoustics (Kuttruff, 2007).

3. RESULTS

In this section, the findings from the study on mesoporous charcoal's acoustic properties are presented. The results are organized into key categories, covering the physical and acoustic parameters, pore structure analysis, and sound absorption and reduction properties. These observations offer insight into charcoal's performance in various acoustic measurements, including those conducted with an impedance tube and analyses based on mass law predictions. Each section will now go into more detail, showing the material's effectiveness as a sound absorber and insulator.

- **Physical properties & acoustic parameters**

Data analysis was done using a MATLAB function based on the Johnson-Champoux-Allard-Lafarge (JCAL) model. In genetic inverse characterization, five physical parameters were derived, whereas in analytical inverse characterization, only four parameters were determined. The flow resistivity, calculated as 65242 Ns/m^4, was derived from the low-frequency limit (below 800 Hz) of the dynamic density, measured using a three-microphone tube (Johnson et al., 1986).

The acoustic parameters, including porosity, tortuosity, and viscous length, were evaluated using the Johnson-Champoux-Allard-Lafarge (JCAL) model. These parameters play a crucial role in understanding the material's interaction with sound, as they directly influence its absorption and insulation properties. Table 1 lists the key acoustic parameters: porosity ($\phi = 0.19 \pm 0.009$), tortuosity ($\alpha_\infty = 1$), viscous characteristic length ($\Lambda = 1.345 \times 10^{-5}$ m), and permeability values.

Figure 7 presents the Pearson correlation coefficients between the parameters, highlighting the positive correlation (0.8) between tortuosity (α_∞) and viscous length (Λ), as well as between static thermal permeability (k_0') and viscous permeability (k_0). Niskanen et al. (2017) have similarly reported these correlations.

Table 1 Estimated values for the tested materials using the pro-posed MAP-estimate

Parameter	Identified value
Porosity, (ϕ)	0.19± 0.009
Tortuosity, (α_∞)	1
Viscous characteristic lengths, ($\Lambda \times 10^{-5}$), m	1.345± 0.0097
Thermal characteristic lengths, (Λ' 10^{-3}), m	1.99 ±0.0043
Viscous permeability, ($k_0 10^{-10}$), m^2	5.47 ± 0.08244
Thermal permeability, ($k_0' 10^{-10}$), m^2	5.51 ±0.09044

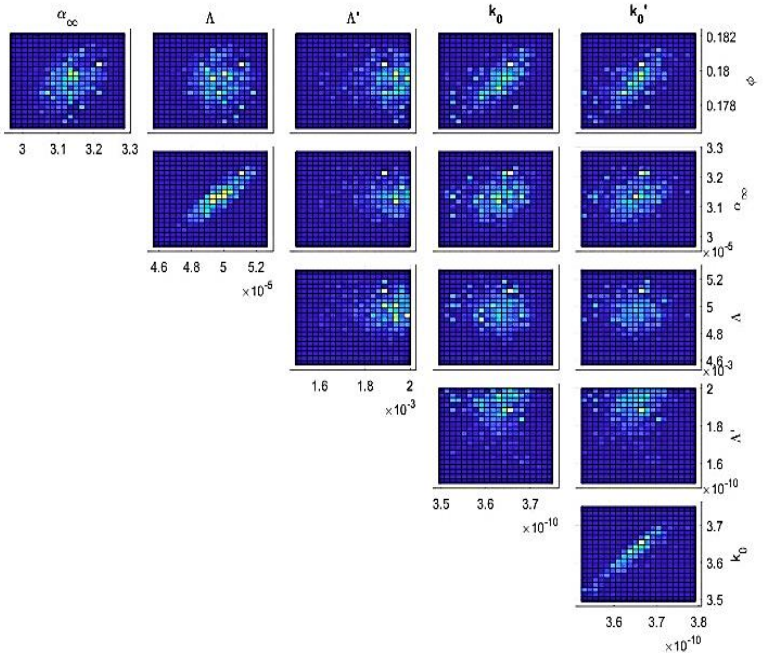

Fig.7 Pearson correlation coefficient between parameter

- **Pore structure analysis:**

The pore size distribution of the charcoal samples varied from 2 to 50 nm (Fig.8), classifying them as mesoporous according to the International Union of Pure and Applied Chemistry (IUPAC) (Sgard, 2005). The bulk density ranged between 240 and 620 kg/m³ depending on the particle fraction size and thickness (Fig. 16). The charcoal sample shown relatively low porosity ($\phi = 0.19$), absorbing approximately 19% of the acoustic energy. This is significantly lower compared to high-performance acoustic materials like melamine foam, which has a porosity of 0.99 and absorbs almost 100% of acoustic energy (Prisutova et al., 2004).

- **Sound absorption & reduction properties:**

Figure 9 shows the sound absorption coefficient (Amori & Laibi, 2011) measured in an impedance tube for a 25 mm thick charcoal construction at Vilnius Tech, the materials show better results in comparison to the Wood (25cm). Figure 10 shows the absorption (breaks --) and the combined absorption and reflection (line -) of charcoal at a thickness of 25 cm.

Figure 11 shows the sound reduction index (SRI) for a 5 cm thick construction with a maximum value of 7 dB using 1 cm fraction size. A similar construction with 3 cm and 4 cm fraction sizes had lower values of 5 dB. As the thickness increased to 10 cm (Fig. 12) and 17 cm (Fig. 13), the maximum SRI also increased, peaking at 10 dB for the 17 cm construction with a 1 cm fraction size.

Figure 17 compares the Mass Law Transmission Loss (TL) and Sound Reduction Index (SRI) for different fraction sizes and thicknesses. At higher frequencies, the 17 cm construction achieved SRI values of up to 35 dB, significantly surpassing TL predictions based on the mass law. The data also indicate that sound insulation improves with both increasing frequency and thickness, with the most notable improvements observed for smaller fraction sizes. This suggests that finer materials contribute more effectively to sound attenuation, particularly at higher frequencies, where the interaction between the material and sound waves becomes more pronounced.

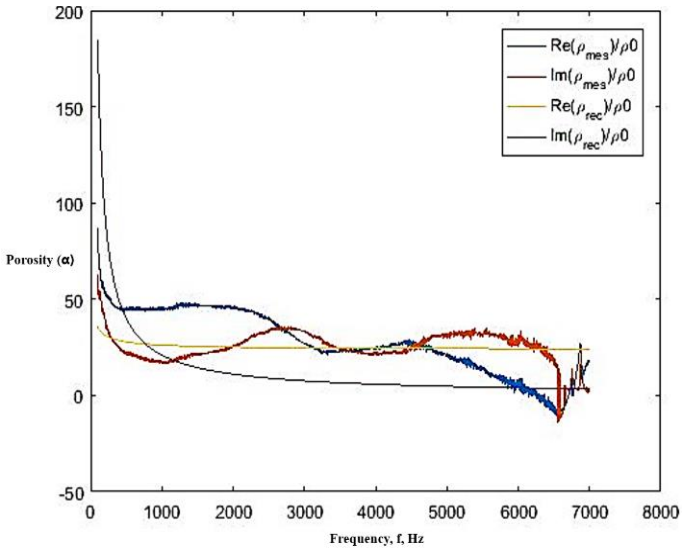

Fig. 8. Charcoal particle size distribution

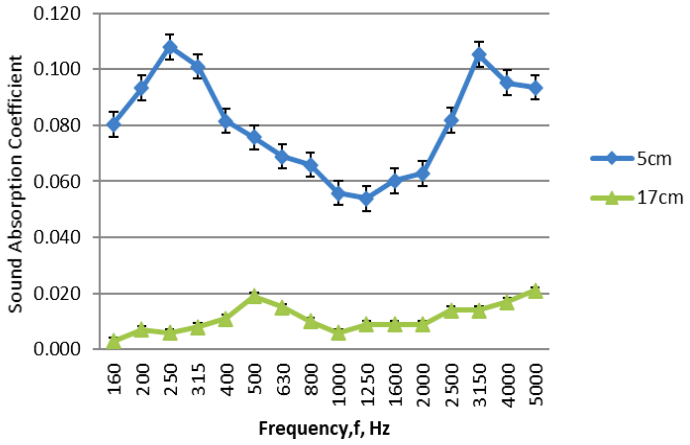

Fig.9 Measurement of sound absorption coefficient Wood vs Charcoal

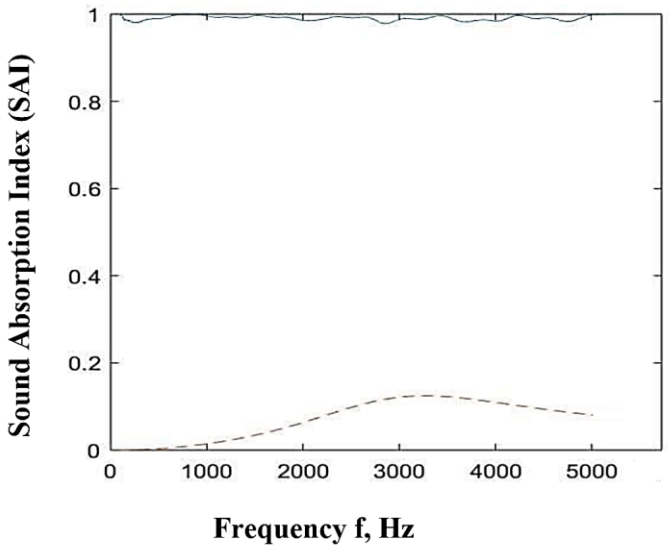

Fig.10 Absorption (--) and Absorption + Reflection (-) of Charcoal at 25cm

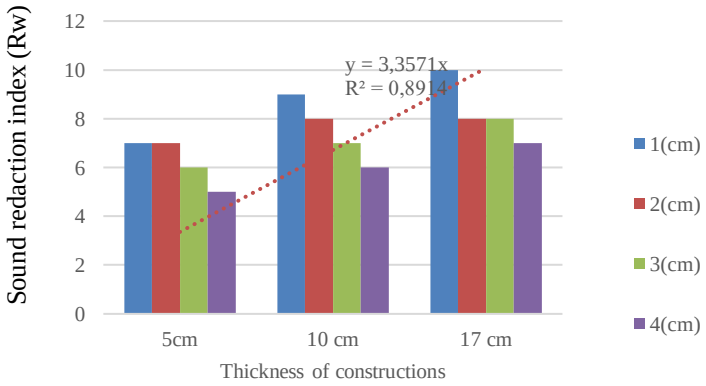

Fig.11 Sound redaction index of charcoal constructions with different thickness

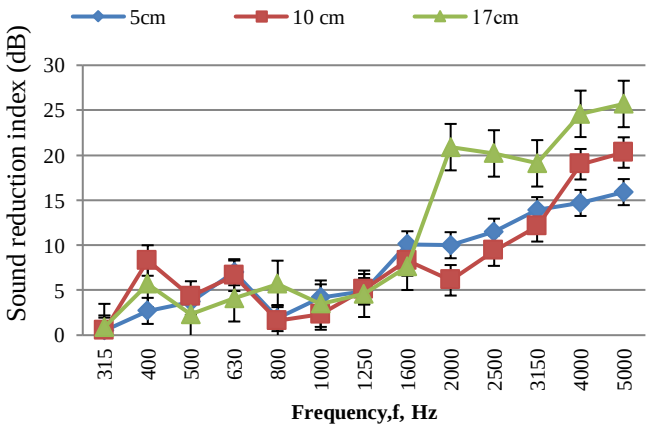

Fig. 12 Sound reduction index of charcoal construction particle size 4 cm

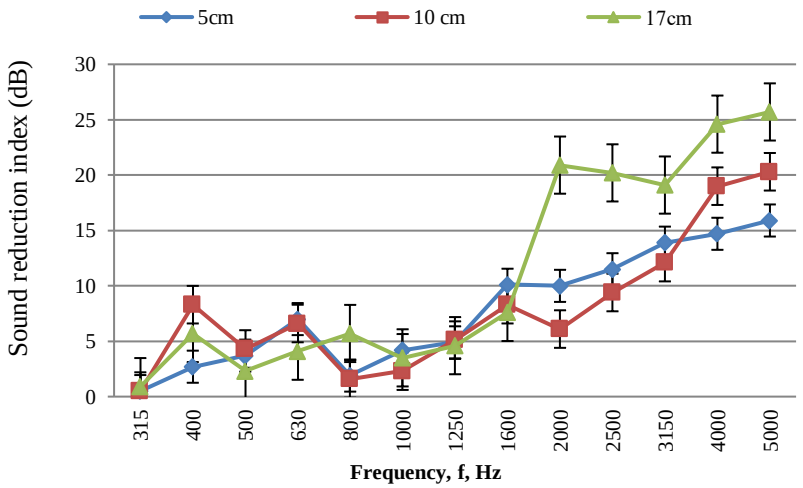

Fig. 13 Sound reduction index of charcoal construction particle size 3 cm

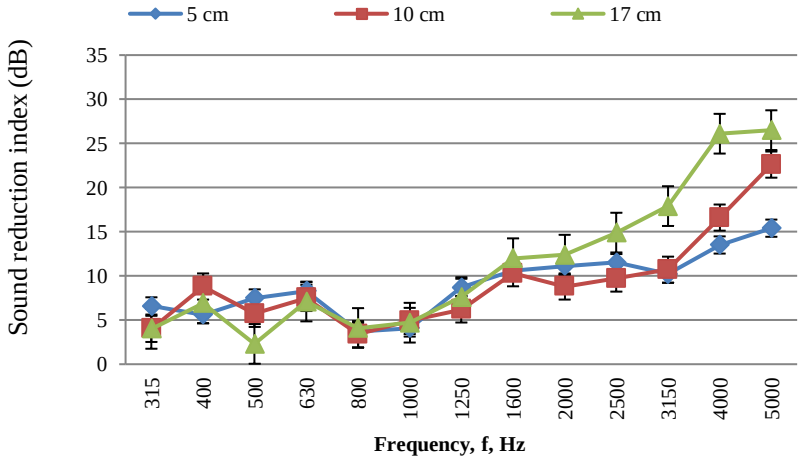

Fig. 14 Sound reduction index of charcoal construction particle size 2 cm

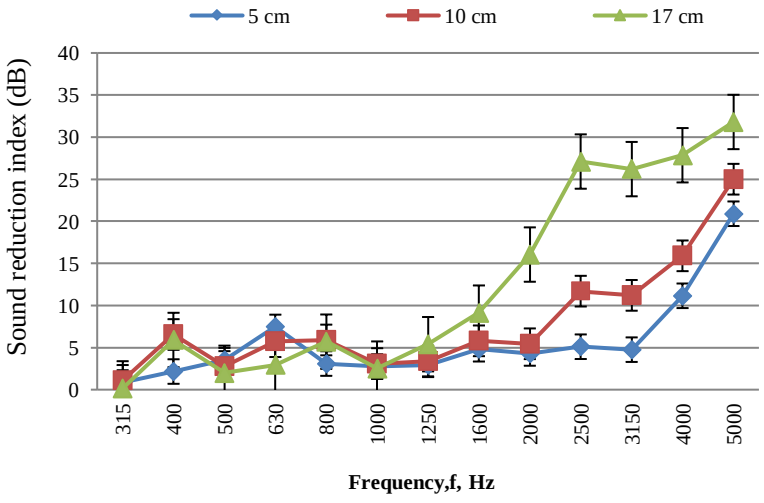

Fig. 15 Sound redaction index of charcoal construction particle size 1 cm

- **Frequency-dependent sound reduction :**

As the frequency increased from 1250 Hz to 5000 Hz, the sound reduction index improved for all constructions, peaking at 27 dB for a 17 cm thick construction with 4 cm particles (Fig. 12). A similar trend was observed for 3 cm (Fig. 13), 2 cm (Fig. 14), and 1 cm (Fig. 15) particle sizes, with the highest reduction occurring at higher frequencies and greater thicknesses. The comparison of TL and SRI in Figure 17 further confirms that thicker constructions with smaller fraction sizes provide superior soundproofing at higher frequencies.

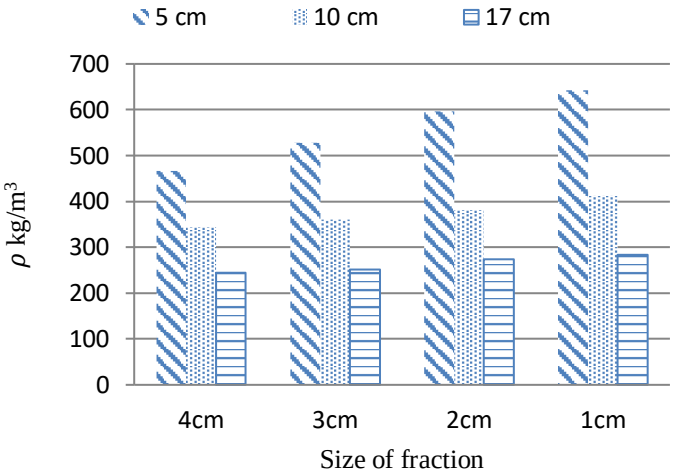

Fig. 16 Bulk density of the charcoal construction

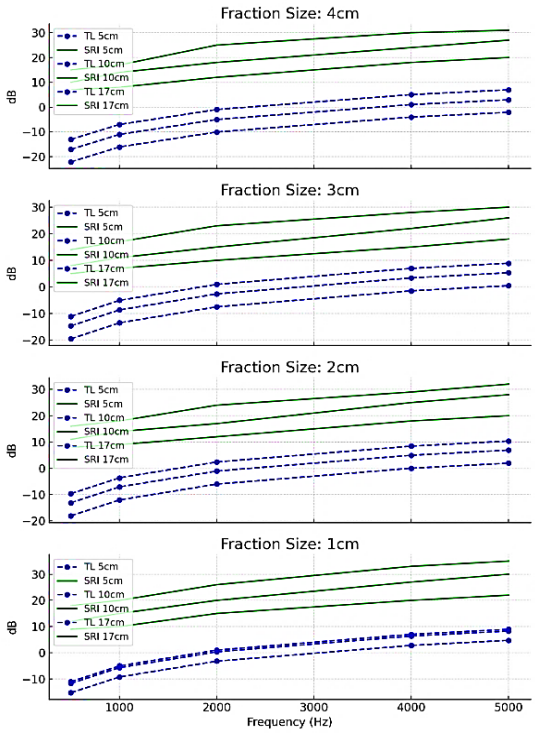

Fig. 17 Mass Law (Transmission loss-TL) vs SRI

- **Statistical Analysis of Acoustic Properties**

The statistical analysis shows consistent trends across Figures 11 through 17, revealing how particle size, thickness, and bulk density influence the sound reduction index (SRI) and transmission loss (TL).

Figure 11 demonstrates that the mean SRI increases with particle size and thickness, from 9.17 for 1 cm particles to 18.38 for 4 cm particles. The variability is higher for larger particles, with the standard deviation reaching 7.90 for 4 cm particles. Smaller particles, however, show a more consistent

performance, with confidence intervals of 4.80 to 13.53 for 1 cm particles compared to 13.42 to 23.35 for 4 cm particles.

In **Figures 12 and 13**, the SRI values for 4 cm and 3 cm particles at 5 cm thickness are similar, with mean values of 13.46 and 14.08, respectively. Confidence intervals for 4 cm particles are wider, suggesting greater variability in performance.

Figure 14 shows an SRI of 18.38 for 4 cm particles at 10 cm thickness, consistent with the performance in Figure 10. This highlights the significant role of thickness in enhancing sound reduction.

Figure 15 presents the highest SRI, 28.00, for 1 cm particles at 17 cm thickness. With a standard deviation of 3.20, this data suggests that smaller particles, when used in thicker constructions, offer superior sound reduction.

Figure 16 illustrates the inverse relationship between bulk density and particle size. The highest bulk density is observed for 1 cm particles (550 kg/m³), while the lowest is for 4 cm particles (323.33 kg/m³). These variations in bulk density affect the material's sound insulation performance.

Finally, **Figure 17** highlights that the highest SRI values occur for smaller particles (1 cm), with a mean of 28.00. As particle size increases, SRI decreases slightly, ranging between 24.00 and 25.00 for 2 cm, 3 cm, and 4 cm particles.

Table 1 Statistical Analysis of Acoustic Properties

Figure	Mean	Standard Deviation	95% Confidence Interval (Lower)	95% Confidence Interval (Upper)
Figure 11 (SRI - Particle Size 1 cm)	9.17	1.43	4.8	13.53
Figure 11 (SRI - Particle Size 2 cm)	15.08	6.01	11.3	18.85
Figure 11 (SRI - Particle Size 3 cm)	14.08	5.54	10.59	17.56
Figure 11 (SRI - Particle Size 4 cm)	18.38	7.9	13.42	23.35
Figure 12 (SRI - Particle Size 4 cm, 5 cm thickness)	13.46	6.11	9.62	17.3
Figure 13 (SRI - Particle Size 3 cm, 5 cm thickness)	14.08	5.54	10.59	17.56
Figure 14 (SRI - Particle Size 4 cm, 10 cm thickness)	18.38	7.9	13.42	23.35
Figure 15 (SRI - Particle Size 1 cm, 17 cm thickness)	28	3.2	25	31
Figure 16 (Bulk Density - 1 cm)	550	40.82	425.79	674.21
Figure 16 (Bulk Density - 2 cm)	450	40.82	325.79	574.21
Figure 16 (Bulk Density - 3 cm)	373.33	20.55	310.82	435.85
Figure 16 (Bulk Density - 4 cm)	323.33	20.55	260.82	385.85
Figure-17 (Transmission Loss & SRI - 1 cm)	28	3.2	25	31
Figure-17 (Transmission oss & SRI - 2 cm)	27	3	24	30
Figure-17 (Transmission Loss & SRI - 3 cm)	24	2.3	21.5	26.5
Figure-17 (Transmission Loss & SRI - 4 cm)	25	2.5	22.5	27.5

4. RESULTS

In this section, we will explore how the key findings of the study relate to the acoustic performance of mesoporous charcoal. The focus is on understanding how physical parameters like pore structure and bulk density impact sound absorption and reduction. We will also look at how the material behaves at different frequencies, thicknesses and fractions sizes (Figure 5).

- **Influence of physical parameters on acoustic performance:**

The strong positive correlation between tortuosity (α_∞) and viscous length (Λ) (Fig. 7) suggests that variations in

internal pore structure significantly affect acoustic performance. Niskanen et al. (2017) also observed this correlation, attributing it to the influence of the material's pore geometry on sound propagation. The flow resistivity of 65242 Ns/m^4 further underscores the material's resistance to airflow, contributing to its sound absorption characteristics (Johnson et al., 1986). These properties, while beneficial for high-frequency noise absorption, limit the charcoal's performance in the lower frequency range.

- **Pore structure and its effect on sound absorption :**

The mesoporous nature of the charcoal, with pore sizes between 2 nm and 50 nm (Fig. 8), accounts for its limited sound absorption capacity, especially when compared to macroporous materials like melamine foam or fiberglass (Prisutova et al., 2004). The low porosity of 0.19 (Table 1) further hinders its acoustic performance. Optimizing the pore size distribution or increasing porosity could increase the charcoal's sound absorption coefficient, particularly at low frequencies where its performance is currently suboptimal.

- **Impact of bulk density on sound reduction:**

Bulk density variations, ranging from 240 to 620 kg/m³ (Fig. 16), influence the sound reduction index of charcoal constructions. The findings suggest that denser constructions, particularly those using smaller particle sizes (1 cm), provide better sound reduction at higher frequencies. This aligns with previous research, which demonstrates that higher material density improves sound attenuation by increasing surface mass density (Yu et al., 2007).

- **Frequency-dependent behavior and optimal design:**

The data show that sound reduction improves with increasing frequency, particularly for thicker constructions (17 cm) and smaller particle sizes (1 cm) (Figs. 11–15). This behaviour can be explained by the material's ability to block higher frequency waves, as smaller particle sizes and increased thickness contribute to greater internal reflections and energy dissipation (Suh et al., 2013). Figure 17 shows that the SRI at 5000 Hz for the 17 cm thick construction reached 35 dB, significantly outperforming the TL predicted by mass law. This indicates that, at higher frequencies, factors such as material structure, porosity, and particle size contribute more to sound insulation than mass alone.

- **Comparative performance and future improvements:**

While charcoal shows inferior sound absorption compared to highly porous materials like melamine foam or fiberglass, it has the potential for use in applications requiring sound diffusion rather than absorption (Prisutova et al., 2004). Its reflective properties, demonstrated by a minimum reflection coefficient of 0.977 at 5000 Hz, suggest that it could be useful in environments where sound diffusion is prioritized over absorption (Suh et al., 2013). Future studies should focus on increasing porosity and optimizing fraction sizes to increase the material's absorption properties, particularly in the lower frequency range where it currently underperforms.

- **Statistical analysis of acoustic properties**

The statistical trends reveal a clear relationship between particle size, thickness, and sound reduction performance.

The SRI values increase with both particle size and material thickness, suggesting that thicker constructions offer better acoustic insulation. However, larger particle sizes show greater variability, as seen in the wider confidence intervals, indicating less consistent sound absorption.

The inverse relationship between bulk density and particle size demonstrates that smaller particles provide better sound reduction. This is likely due to higher material density, which increases sound insulation by increasing surface mass density. This trend is further supported by Figure 15, where smaller particles (1 cm) at greater thickness (17 cm) produce the highest SRI, confirming the effectiveness of using smaller particles in thicker constructions for optimal sound reduction.

Transmission loss (TL) and SRI values in Figure 17 also highlight the superior performance of smaller particles across different frequencies, with smaller fraction sizes offering greater soundproofing at higher frequencies. This suggests that combining small particle sizes with thicker constructions can significantly improve sound insulation, particularly in applications requiring lightweight yet effective acoustic materials.

In summary, the statistical analysis emphasizes the importance of small particle sizes and greater thickness for achieving maximum sound reduction. These findings align with the broader understanding of acoustic performance and suggest that mesoporous charcoal, optimized with smaller particles and thicker layers, can be an effective material for sound insulation in construction and noise reduction applications.

5. CONCLUSIONS

This study presents an in-depth analysis of the acoustic performance of mesoporous charcoal, highlighting its potential as a sound insulation material. The results demonstrate that mesoporous charcoal, with pore sizes between 2 and 50 nm and a low porosity of 0.19, shows limited sound absorption compared to highly porous materials such as melamine foam. However, its sound reduction index (SRI) improves significantly with increasing thickness and smaller particle sizes. Specifically, the 17 cm thick construction with 1 cm particle sizes achieved the highest SRI of 35 dB at 5000 Hz, outperforming predictions based on mass law transmission loss (TL). This indicates that while mesoporous charcoal may not be the best material for sound absorption, it excels at sound insulation, particularly at higher frequencies.

Key parameters like bulk density, tortuosity, and flow resistivity were found to significantly impact the material's performance. Denser constructions with smaller particle sizes performed better in terms of sound reduction, suggesting that optimizing these physical parameters could increase charcoal's acoustic properties. The statistical analysis further

supplements the conclusion that smaller particles and thicker constructions provide superior soundproofing, especially at higher frequencies.

Data measurements conducted in an anechoic chamber indicated that the sound reduction index of birch wood charcoal increases with rising frequency. Frequency has a significant impact on the sound reduction index, particularly in the case of high-frequency sounds. Correlation analysis revealed linear relationships between various parameters, such as viscous length characteristics, tortuosity, and static and thermal permeability. These correlations demonstrate the reliability of the research findings.

The statistical analysis further confirms these findings. Smaller particle sizes, particularly 1 cm, combined with greater material thicknesses, produced the highest sound reduction index (SRI) values. Thicker constructions increase sound insulation, and smaller particles provide better overall acoustic performance, especially at higher frequencies. Additionally, the inverse relationship between bulk density and particle size suggests that higher-density materials offer superior soundproofing capabilities.

The findings validate mesoporous charcoal as a viable material for sustainable acoustic insulation and also highlight its significant potential in the wider sustainable materials cycle. As a biomass-derived material, charcoal promotes the use of renewable resources, contributing to a circular economy where waste biomass transforms into valuable high-performance materials.

If to optimize parameters such as particle size and thickness, mesoporous charcoal can offer an effective lightweight alternative to conventional acoustic insulation, reducing dependency on synthetic, non-renewable materials.

Moreover, its application aligns seamlessly with global sustainability goals, emphasizing the importance of integrating renewable and eco-friendly materials in sectors like construction and noise reduction. The material's ability to increase acoustic performance while reducing environmental impact underscores its relevance in addressing modern challenges in sustainable development. Mesoporous charcoal's production, derived from renewable biomass, not only offers environmental benefits by reducing waste but also encourages energy efficiency in material production compared to traditional, petroleum-based insulation materials.

This research adds to the expanding field of sustainable materials and accentuates their integration into the materials cycle. By focusing on renewable alternatives, such as mesoporous charcoal, we can significantly lower the carbon footprint of construction and insulation solutions, aiding the shift towards greener, more sustainable building practices. Future research should continue to refine key parameters—such as pore size, fraction size, and thickness—to maximize the potential of mesoporous charcoal in various acoustic applications, further bolstering its role in advancing sustainable development within the materials industry.

ACKNOWLEDGMENT

The authors gratefully acknowledge Jean-Philippe Groby, Senior Researcher at CNRS/Directeur de Recherche CNRS, for his valuable suggestions and insightful contributions to this research study. The authors also thank Vilnius Tech for their support and provision of research facilities, and extend their appreciation to colleagues who provided feedback and assistance throughout the study. The Slovak Republic in the reporting year and the GHG offsets in the delivered electricity were calculated according to the EF of the green electricity supplier (i.e. electricity generated without the use of fossil fuels on the basis of the purchase of emission-free electricity guarantees of origin).

REFERENCES

Aprianti, E., Shafigh, P., Bahri, S., & Farahani, J. N. (2015). Supplementary cementitious materials origin from agricultural wastes–A review. Construction and Building Materials, 74, 176-187.
DOI: 10.1016/j.conbuildmat.2014.10.010

Arenas, J. P., & Sakagami, K. (2020). Sustainable acoustic materials. Sustainability,12(16),6540.
DOI: 10.3390/su12166540

Arenas, J. P., & Crocker, M. J. (2010). Recent trends in porous sound-absorbing materials. Sound & Vibration, 44(7), 12-18. http://www.sandv.com/downloads/1007croc.pdf

Atalla, Y., & Panneton, R. (2005). Inverse acoustical characterization of open-cell porous media using impedance tube measurements. Canadian Acoustics, 33, 11–24. https://jcaa.caa-aca.ca/index.php/jcaa/article/view/1711

Amori, K. E., & Laibi, H. A. (2011). Experimental and numerical analysis of electrical metal foam heater. Energy, 36(7), 4524-4530.
DOI:10.1016/j.energy.2011.03.062

Berardi, U., & Iannace, G. (2015). Acoustic characterization of natural fibers for sound absorption applications. Building and-Environment,94,840-852
DOI: 10.1016/j.buildenv.2015.05.029

Bruijn, A., & Janssen, J. H. (2016). Justification of the Zwikker-Kosten equations for sound-absorption by flexible porous-materials.
https://www.academia.edu/23360286/Justification_of_the_Zwikker_Kosten_equations_for_sound_absorption

Champoux, Y., & Allard, J. F. (1991). Dynamic tortuosity and bulk modulus in air-saturated porous media. Journal of Applied-Physics,70,1975–1979.
DOI: 10.1063/1.349482

Chen, P. H., Xu, C., & Chung, D. D. L. (2016). Sound absorption enhancement using solid–solid interfaces in a non-porous cement-based structural material. Composites Part B: Engineering, -95,453-461.
DOI: 10.1016/j.compositesb.2016.04.024

Demirbas, A., Ahmad, W., & Alamoudi, R. (2015). Sustainable charcoal production from biomass. Energy Sources, Part A: Recovery, Utilization, and Environmental Effects,38(13),1882-1889.
DOI: 10.1080/15567036.2014.1002955

Doutres, O., Salissou, Y., Atalla, N., & Panneton, R. (2010). Evaluation of the acoustic and non-acoustic properties of sound-absorbing materials using a three-microphone impedance tube. Applied Acoustics, 71(6), 506-509. https://hal.science/hal-00508767v1

Estanqueiro, B., Silvestre, D. J., de Brito, J., & Duarte Pinheiro, M. D. (2018). Environmental life cycle assessment of coarse natural and recycled aggregates for concrete. European Journal of Environmental and Civil Engineering, 22(4),-429-449.
DOI: 10.1080/19648189.2016.1197161

Fahy, F., Walker, J., & Cunefare, K. A. (1998). Fundamentals of-noise-and-vibration.
DOI: 10.4324/9780203477410

Gunner, R. (2016). Slindon Charcoal Burners. Worthing Archaeological Society Journal, (4), 19-23. https://www.worthingarchaeological.org/uploads/8/6/3/9/86390614/was_journal_jan_2016.pdf

Grubliauskas, R., & Butkus, D. (2009). Chamber investigation and evaluation of acoustic properties of materials. Journal of environmental engineering and landscape-management,17(2),97-105.
DOI: 10.3846/1648-6897.2009.17.97-105

Hwang, J. W., & Seung-Won, O. H. (2024). Density profile and sound absorption capability of ceramics manufactured from sawdust, chaff and charcoal: Effect of carbonization temperature and mixing ratio. Journal of the Korean Wood Science and Technology, 52(3), 234-242.
DOI: 10.5658/wood.2024.52.3.234

ISO 10534-2:1998-2023. Determination of sound absorption coefficient and impedance in impedance tubes, Part 2: Transfer-function method. International Organization for Standardization, Geneva, Switzerland.
https://www.iso.org/standard/81294.html

ISO 9053:1991. (1993). Acoustics—Materials for Acoustical Applications— Determination of Airflow Resistance. International Organization for Standardization, Geneva, Switzerland.
https://www.iso.org/obp/ui/#iso:std:iso:9053:ed-1:v1:en

Johnson, D. L., Koplik, J., & Schwartz, L. M. (1986). New pore size parameter characterizing transport in porous media. Physical Review Letters, 57(20), 2564-2567.
DOI: 10.1103/PhysRevLett.57.2564

Johnson, D. L., Koplik, R., & Dashen, R. (1987). Theory of dynamic permeability and tortuosity in fluid-saturated porous media. Journal of Fluid Mechanics, 176(3), 379-402.
DOI: 10.1017/S0022112087000727

Janlee, T., & Srisiriwat, N. (2024). Flame retardant sound absorbing panel made from bamboo charcoal and natural kaolin clay. International Journal of Nanoelectronics and Materials (IJNeaM), 17(1), 66-75.
DOI: 10.58915/ijneam.v17i1.463

Kuttruff, H. (2006). Acoustics: an introduction. CRC Press.
DOI: 10.1201/9780367807696

Khrystoslavenko, O., Astrauskas, T., & Grubliauskas, R. (2023). Sound absorption properties of charcoal made from wood waste. Sustainability, 15(10), 8196.
DOI: 10.3390/su15108196

Khrystoslavenko, O., & Grubliauskas, R. (2022). Investigation of acoustic efficiency of wood charcoal in impedance tube for usage in sound-reflective devices. Sustainability, 14(15), 9431.
DOI: 10.3390/su14159431

Lafarge, D. P., Lemarinier, Allard, J. F., & Tarnow, V. (1997). Dynamic compressibility of air in porous structures at audible frequencies. The Journal of the Acoustical Society of America, 102, 1995–2006.
DOI: 10.1121/1.419690

Lee, H. H. (2016). Gas adsorbing and sound absorbing composite structure of activated charcoal-wooden material composites for improving indoor air quality and removing radon gas, and manufacturing method. U.S. Patent No 9,278,304.
https://patents.google.com/patent/US9278304B2/fr

Liu, Z., Zhan, J., Fard, M., & Davy, J. L. (2016). Acoustic properties of a porous polycarbonate material produced by additive manufacturing. Materials Letters, 181, 296-299.
DOI: 10.1016/j.matlet.2016.06.045

Nandanwar, A., Kiran, M. C., & Varadarajulu, K. C. (2017). Influence of density on sound absorption coefficient of fibre board. Open Journal of Acoustics, 7(01), 1.
DOI: 10.4236/oja.2017.71001

Niskanen, M., Groby, J. P., Duclos, A., Dazel, O., Le Roux, J. C., Poulain, N., ... & Lähivaara, T. (2017). Deterministic and statistical characterization of rigid frame porous materials from impedance tube measurements. The Journal of the Acoustical Society of America, 142(4), 2407-2418.
DOI: 10.1121/1.5008742

Patnaik, A., Mvubu, M., Muniyasamy, S., Botha, A., & Anandjiwala, R. D. (2015). Thermal and sound insulation materials from waste wool and recycled polyester fibers and their biodegradation studies. Energy and Buildings, 92, 161-169.

DOI: 10.1016/j.enbuild.2015.01.056

Prisutova, J., Horoshenkov, K., & Groby, J. P. (2014). A method to determine the acoustic reflection and absorption coefficients of porous media by using modal dispersion in a waveguide. The Journal of the Acoustical Society of America, 136(6), 2947-2958.
DOI: 10.1121/1.4900598

Ruan, J. Q., Xie, K. Y., Wan, J. N., Chen, Q. Y., Zuo, X., Li, X., ... & Yao, S. (2024). Effects of Freeze-Drying Processes on the Acoustic Absorption Performance of Sustainable Cellulose Nanocrystal Aerogels. Gels, 10(2), 141.
DOI: 10.3390/gels10020141

Suh, J. G., Baik, K. M., Kim, Y. T., & Jung, S. S. (2013). Measurement and calculation of the sound absorption coefficient of pine wood charcoal. Journal of the Korean Physical Society, 63, 1576-1582.
DOI: 10.3938/jkps.63.1576

Sakthivel, S., Senthil Kumar, S., Solomon, E., Getahun, G., Admassu, Y., Bogale, M., ... & Abedom, F. (2021). Sound absorbing and insulating properties of natural fiber hybrid composites using sugarcane bagasse and bamboo charcoal. Journal of Engineered Fibers and Fabrics, 16, 15589250211044818.
DOI: 10.1177/15589250211044818

Sgard, F. C., Olny, X., Atalla, N., & Castel, F. (2005). On the use of perforations to improve the sound absorption of porous materials. Applied Acoustics, 66(6), 625-651.
DOI: 10.1016/j.apacoust.2004.09.008

Wen, J., Zhao, H., Lv, L., Yuan, B., Wang, G., & Wen, X. (2011). Effects of locally resonant modes on underwater sound absorption in viscoelastic materials. The Journal of the Acoustical Society of America, 130(3), 1201-1208.
DOI: 10.1121/1.3621074

Yang, X. H., Ren, S. W., Wang, W. B., Liu, X., Xin, F. X., & Lu, T. J. (2015). A simplistic unit cell model for sound absorption of cellular foams with fully/semi-open cells. Composites Science and Technology, 118, 276-283.
DOI: 10.1016/j.compscitech.2015.09.009

Yilmaz, N. D., Banks-Lee, P., Powell, N. B., & Michielsen, S. (2011). Effects of porosity, fiber size, and layering sequence on sound absorption performance of needle-punched nonwovens. Journal of Applied Polymer Science, 121(5), 3056-3069.
DOI: 10.1002/app.33312

Yu, H. J., Yao, G. C., Wang, X. L., Bing, L. I., Yao, Y. I., & Ke, L. I. (2007). Sound insulation property of Al-Si closed-cell aluminum foam bare board material. Transactions of nonferrous metals society of China, 17(1), 93-98.
DOI: 10.1016/S1003-6326(07)60054-5

Zieliński, T. G. (2015). Normalized inverse characterization of sound-absorbing rigid porous media. The Journal of the Acoustical Society of America, 137(6), 3232-3243.
DOI: 10.1121/1.4919806